Adiabatic dynamical-decoupling-based control of nuclear spin registers

O. T. Whaites [1], J. Randall [2,3], T. H. Taminiau [2,3] and T. S. Monteiro [1]

[1] *Department of Physics and Astronomy, University College London, Gower Street, London WC1E 6BT, United Kingdom*

[2] *QuTech, Delft University of Technology, P.O. Box 5046, 2600 GA Delft, Netherlands*

[3] *Kavli Institute of Nanoscience Delft, Delft University of Technology, P.O. Box 5046, 2600 GA Delft, Netherlands*

(Received 26 June 2021; revised 2 January 2022; accepted 22 February 2022; published 21 March 2022)

The use of the nuclear spins surrounding electron spin qubits as quantum registers and long-lived memories opens the way to new applications in quantum information and biological sensing. Hence, there is a need for generic and robust forms of control of the nuclear registers. Although adiabatic gates are widely used in quantum information, they can become too slow to outpace decoherence. Here, we introduce a technique whereby adiabatic gates arise from the dynamical decoupling protocols that simultaneously extend coherence. We illustrate this pulse-based adiabatic control for nuclear spins around NV centers in diamond. We obtain a closed-form expression from Landau-Zener theory and show that it reliably describes the dynamics. By identifying robust Floquet states, we show that the technique enables polarization, one-shot flips, and state storage for nuclear spins. These results introduce a control paradigm that combines dynamical decoupling with adiabatic evolution.

DOI: 10.1103/PhysRevResearch.4.013214

I. INTRODUCTION

There is enormous interest in the development of quantum technologies based on spins in the solid state. Optically active defects, such as the nitrogen vacancy (NV) center in diamond, offer well-isolated individual electronic spins with long coherence times, optical addressability, and operation from cryogenic to room temperatures [1–7]. In combination with nearby coupled nuclear spins, these systems provide a multiqubit platform with a wide range of applications including detection, imaging, and atomic-scale characterization of the spin samples [8–12], quantum computation, and quantum networks [13–15].

Both sensing and quantum information applications typically rely, for control of the central electronic spin, on sequences of periodically repeated microwave pulses, known as dynamical decoupling (DD). Although DD was initially employed to decouple the central electron spin qubit from the decohering effect of the surrounding spin bath [16], it was soon recognized that the same sequences could also be used to sense individual nuclear spins [17,18]. For the case of the NV center in diamond, the entanglement generated between the electron spin and the $I = 1/2$ ^{13}C nuclear spins is being explored as a tool for control, with nuclear spins as multiqubit registers and quantum memories [19,20]. Furthermore, state storage in nuclear spins has been used to augment protocols for quantum sensing and nanoscale Nuclear Magnetic Resonance (NMR) [21]. Adiabatic quantum gates are well-established in quantum information but, as adiabaticity entails slow parameter sweeps, outpacing decoherence represents a problem [22]. Proposals employing DD to extend coherence *alongside* the adiabatic gates have been investigated [23,24].

However, to our knowledge, the gates exploiting adiabatic passage in eigenstates intrinsic to the common pulse-DD protocols have not previously been considered: this may be surprising as they offer the additional advantage that coherence protection from pulse-DD comes for free. So here we introduce and investigate a technique that combines adiabatic passage (thus enabling nuclear qubit gates) with coherence protection (of the central electronic qubit) through DD. We name this method ad-Pulse.

We show that this type of control is quite generic and, for various applications, does not require knowledge of the individual resonances. ad-Pulse can also be applied to a many-spin bath and we show some applications are insensitive to the number of spins. We illustrate ad-Pulse using the example of an NV center and surrounding nuclear registers. We show also that it may polarize and initialize small nuclear clusters and investigate possibilities for quantum state storage and readout.

In Sec. II, we briefly review pulse-based DD, including polarization protocols. We discuss key differences with standard DD and describe the implementation of ad-Pulse. Since ad-Pulse is most clearly understood as adiabatic passage, but in the underlying Floquet eigenspectra, in Sec. III, we review Floquet theory applied to dynamical decoupling. We illustrate ad-Pulse by showing how adiabatic passage along a Floquet state allows a one-sweep flip of the entire nuclear bath. In Sec. IV, we apply Landau-Zener (LZ) theory to ad-Pulse, but in the space of Floquet eigenstates. We derive a closed form expression that accurately matches exact numerics. Equation (4) is a central result of this paper: It offers an independent check on the robustness of the adiabatic analysis, fully containing dependence on all experimentally chosen parameters;

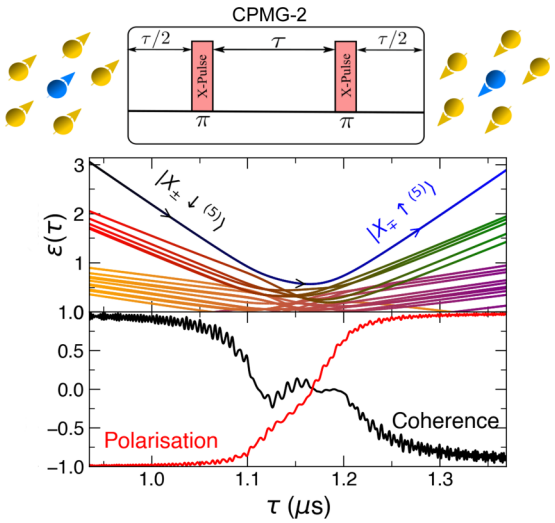

FIG. 1. Adiabatic dynamical decoupling (ad-Pulse) illustrated for an NV spin surrounded by nuclear spins. Top panel: The common CPMG-2 pulse sequence. For typical pulse-based control, the sequence is reapplied over N_p cycles, at a pulse spacing $\tau_r \sim \pi/\omega_L$ fixed for each initialization of the NV spin state. For ad-Pulse, τ is instead swept slowly from cycle to cycle, through the region $\tau \sim \tau_r$. Lower panel: For an NV spin prepared in a coherent $|X^+\rangle$ state and spin bath initially in the $|\downarrow^{(5)}\rangle$ state (five spin example chosen, but effect is generic), the sweep flips the entire bath to the $|\uparrow^{(5)}\rangle$ state (red line) while the NV qubit passes through an entangled state for $\tau \sim \tau_r \approx 1.15\,\mu$s then recovers coherence at the endpoint (black line). Middle panel: The corresponding Floquet eigenphases $\mathcal{E}(\tau)$ and shows one may visualize the process as adiabatic passage, albeit in the associated Floquet eigenphase spectrum. Other applications, starting even from initial mixed thermal nuclear states, are also investigated here.

it enables one to determine what step sizes optimize the trade-off between a slow sweep (required for adiabatic passage) and high speed gates (to protect coherence). Detailed derivations are presented in the Appendix. In Sec. V, we consider the application of ad-Pulse to nuclear polarization and present comparisons with LZ theory [Eq. (4)]. We investigate initialization of surrounding nuclear registers. In Sec. VI, we consider the application to qubit gates based on adiabatic passage. Finally, in Sec. VII, we discuss the results and conclude.

II. DYNAMICAL DECOUPLING

An NV electron spin system surrounded by $N_{\rm nuc}$ nuclear spins is described by the Hamiltonian

$$\hat{H}(t) = \hat{H}_p(t) + \omega_{\rm L} \sum_n \hat{I}_z^{(n)} + \hat{S}_z \sum_n \mathbf{A}^{(n)} \cdot \hat{\mathbf{I}}^{(n)}. \qquad (1)$$

$\hat{H}_p(t) = \Omega(t)\hat{S}_x$ is the pulse control Hamiltonian (in a frame rotating at the frequency of the microwave pulse). $\Omega(t)$ is the microwave drive strength which is nonzero only during the pulses. For the CPMG-2 protocol, microwave π pulses are applied along the x axis at regular equally spaced intervals, τ. This is illustrated in Fig. 1. The pulse duration for a π flip of the electron spin is denoted T_π. $\omega_{\rm L}$ is the nuclear Larmor frequency; the hyperfine field $\mathbf{A}^{(n)}$ felt by the nuclear spin has components $A_\perp^{(n)}, A_z^{(n)}$ relative to the z axis. We take $A_\perp^{(n)} \equiv A_x^{(n)}$. Other protocols can involve more intricate combinations of pulses, but we can illustrate the general behavior using the simple CPMG protocol.

N_p cycles of the chosen protocol are applied. An insightful semiclassical model considers the effect of a DD protocol as a filter function $F(\omega)$, peaked near $\omega = \pi/\tau$. The width of $F(\omega)$ in frequency $\propto \frac{1}{N_p\tau}$, hence as N_p increases, the filter function becomes sharply peaked about an ever narrower range of frequencies centered at a resonant $\tau \simeq \tau_r$. The central qubit is insensitive to magnetic noises at frequencies outside this range. Nuclear spins surrounding the central NV are a source of magnetic dephasing noise at $\omega \simeq \omega_L \simeq \pi/\tau_r$. Away from $\tau \approx \tau_r$, the NV coherence time T_2 is greatly enhanced. In a corresponding quantum bath picture, if the chosen pulse interval corresponds to $\tau \simeq \pi/\tau_r$, the central qubit and nuclei interact and entangle, leading to decoherence.

For CPMG-2, the resonant pulse spacing is $\tau_r = j\pi/(\omega_L + A_z^{(n)}/2)$, where j is an odd integer (below we omit the n superscript when discussing a single-nuclear spin case and unless specified discuss the lowest harmonic $j = 1$). Notably, the dependence on A_z means that, in fact, different nuclear spins have different τ_r and are not all at the Larmor frequency ω_L. Hence, the observed comb of resolved coherence dips represents a resource for sensing and characterization of the nuclear spins. In addition, the electronic -nuclear entanglement at τ_r has recently even turned DD into an invaluable toolbox for efficient control and manipulation of nuclear qubits, mediated by the central NV spin.

A. Pulse-based polarization protocols

Recently proposed pulse protocols with resonances that are state selective represent an interesting offshoot of DD. Typically, they yield a pair of resonances $\tau_r \equiv \tau_r^{\pm}$ that are resonant only with either an up or down nuclear spin state. For instance, PulsePol [25], proposed in 2018, is a robust multipulse sequence combining π and $\pi/2$ pulses, $[\frac{\pi_y}{2} - \tau - \pi_{-x} - \tau - \frac{\pi_y}{2}\frac{\pi_x}{2} - \tau - \pi_y - \tau - \frac{\pi_x}{2}]^{2N_p}$ repeated over $2N_p$ cycles. For pulse spacings $\tau_r \simeq j\pi/(2\omega_I)$, where $j = 1, 3...$ it yields an effective flip-flop Hamiltonian $\hat{H}_{\rm PP} = gI^{\pm}S^{\mp}$. Hence, each of the components flips only one nuclear spin state.

PolCPMG [26,27], also proposed in 2018, is a variant of CPMG, obtained by applying an over-/underrotation to the pulses, i.e., $\theta = (1 + \delta\theta)\pi$ where $\delta\theta = 0$ corresponds to CPMG. It was also shown experimentally to hyperpolarize a nuclear bath [27] for $\delta\theta \simeq 0.05 - 0.25\pi$. Another polarization protocol, TOP-DNP, proposed and investigated experimentally in Ref. [28] for NMR considers small angles $\theta = \delta\theta \ll \pi$ as qubit coherence protection is not the aim.

Further details including respective values of τ_r are given in the Appendix but both PulsePol and PolCPMG have been experimentally investigated using NV centres. If the objective is polarization of the nuclear bath, it is advantageous to reinitialize the NV qubit and repeatedly apply the N_p cycles. N_r is the number of repetitions at a given τ. The coherence time T_2 of the NV is only of interest over the N_p cycle run, since for each repetition $r = 1, 2, 3...N_r$ there is optical reinitialization: the NV state (e.g., $|X^{\pm}\rangle$ for PolCPMG) is prepared anew.

Full understanding of DD resonance behavior benefits from a full quantum bath analysis. While there are several approaches, it has been shown that the loss of coherence identified in DD studies at resonances correspond to avoided crossings of the underlying Floquet eigenstates [26,27,29,30] and such Floquet spectroscopy offers an insightful pictorial description. ad-Pulse, as we will see, may be viewed simply as adiabatic passage over one or more of these avoided crossing regions. We now describe specifically how to implement ad-Pulse.

B. Implementation of adiabatic DD: ad-Pulse

In standard DD, the pulse spacing is set at τ and then N_p cycles of the protocol are applied. The duration of each protocol is $T = m_p\tau$, with $m_p = 2$ for CPMG-2, $m_p = 4$ PulsePol (for simplicity, pulse duration is included in τ). The NV is then reinitialized optically before the next value of τ. Hence, each different τ corresponds to a different, completely independent experiment.

In contrast, ad-Pulse instead sweeps over a range $\Delta\tau$ of pulse spacings *without reinitialization*, in $k = 1, ...N_s$ steps. Thus, $\tau_{k+1} = \tau_k + \delta\tau$ where $\delta\tau$ is the step size. Starting from an initial $\tau = \tau_{\rm ini}$, $\tau_k = \tau_{\rm ini} + (k-1)\delta\tau$. The actual sequence time up to step k is $t_k = \sum_{l=1}^{l=k} m_p\tau_l$, hence

$$t_k = \sum_{l=1}^{l=k} m_p\tau_l = m_p k[\tau_{ini} + (k-1)\delta\tau/2]. \tag{2}$$

For an estimate of the sweep time, we can take $t_{k=N_s} \sim m_p N_s\overline{\tau}$ with $\overline{\tau} = \tau_{\rm ini} + N_s\delta\tau/2$. To understand the resulting dynamics, we now consider Floquet theory.

III. FLOQUET PICTURE

Floquet theory is well-established in many fields in physics, mostly relating to continuous driving, including applications in NMR [31]. However, the term covers a wide range of scenarios: The Floquet theorem is applicable to any temporally periodic system. For a system with a temporally periodic Hamiltonian, $\hat{H}(t+T) = \hat{H}(t)$, Floquet's theorem allows one to write solutions of the Schrödinger equation in terms of quasienergy states $|\psi_l(t)\rangle = \exp(-i\epsilon_l t)|\Phi_l\rangle$, where ϵ_l is the quasienergy, $|\Phi_l(t)\rangle = |\Phi_l(t+T)\rangle$, T is the period, and $l = 1, .., D$ (D is the dimension of the state space).

If we require only stroboscopic knowledge of our system at times $t = t + kT$, one may obtain eigenstates of the one-period unitary evolution operator $\hat{U}(T) \equiv \hat{U}(T, 0)$ for the joint electron-nuclear spin bath system under pulse-DD. The Floquet states $|\Phi_l\rangle$ obey the eigenvalue equation

$$\hat{U}(T)|\Phi_l\rangle = \lambda_l|\Phi_l\rangle \equiv \exp(-i\mathcal{E}_l)|\Phi_l\rangle, \tag{3}$$

where $\mathcal{E}_l \equiv \tan^{-1}{\rm Im}\,\lambda_l/{\rm Re}\,\lambda_l$ is the eigenphase (the Floquet phase).

One important application is so-called Floquet engineering (FE) [32], where a system continuously driven by a typically strong or high-frequency field can be shown to correspond to an effective, static Hamiltonian with renormalized parameters by averaging over the period of the driving. By varying the *amplitude* of the off-resonant drive, one may tune over the effective Hamiltonian. This approach has been proposed theoretically for polarization of a nuclear spin bath [33] using an adiabatic sweep of the energy eigenvalues of an effective static Hamiltonian.

The ad-Pulse proposed here is quite distinct from FE: there is no period averaging and in fact its unique characteristic is that one sweeps coherently over *period* T of the pulse protocol, within a range containing the characteristic resonances of the nuclear spins of interest. In contrast, FE methods modulate the amplitude of the drive. We emphasise that for ad-Pulse, the microwave frequency $\omega_{\rm mw}$ during the short pulses plays no role in determining adiabaticity. The pulses are not altered, and by working in the rotating frame, dependence on $\omega_{\rm mw}$ has been eliminated. The timescale of interest is far slower, $\sim 2\pi/T \ll \omega_{\rm mw}$, than for studies of the microwave driving.

Previously, it has been shown that the loss of coherence identified in DD studies at resonances correspond to avoided crossings of the underlying Floquet eigenphases [29,30]. Recognizing this, ad-Pulse sweeps adiabatically over the Floquet eigenphases instead: If sufficiently slow, the sweep follows a Floquet eigenstate adiabatically and coherently, in a process analogous to adiabatic passage using usual energy eigenstates. An example is presented below.

A. Example: Whole bath flip by ad-Pulse

In Fig. 1, we illustrate an application of ad-Pulse using CPMG-2. We consider a bath of five nuclear spins, C1,C2...C5 (couplings tabulated in the Appendix) from a cluster employed as registers in recent experiments in Ref. [20], with $A_x/(2\pi)$ within the range [20 : 60] kHz.

The Floquet eigenphases $\mathcal{E}_l \equiv \mathcal{E}_l(\tau)$ are obtained numerically by diagonalizing the matrix $\hat{U}(T)$ for the full spin cluster. The eigenvalues $\mathcal{E}_l$, are plotted over a range centered around $\tau = \pi/\omega_L$ for $B_0 = 0.0403$ T. We plot $\mathcal{E}_l \in [-\pi : \pi]$, noting the spectra are multiply degenerate under the shift $\mathcal{E}_l \to \mathcal{E}_l + 2\pi n$, for integer n [30].

We find that an interesting and useful feature of the Floquet spectra of CPMG-2, for arbitrary number of of nuclei $N_{\rm nuc}$, is the existence of a gap between either of the extremal states (those that asymptotically tend to maximal/minimal polarized states $M_z = \pm N_{\rm nuc}/2$) and all remaining M_z manifolds. Each and every one of the states in the adjoining $M_z = \pm(N_{\rm nuc}/2 - 1)$ manifolds experiences a coupling $A_x^{(n)}\hat{I}_x^{(n)}\hat{S}_z$ associated with an anticrossing [30]—and level repulsion—with the extremal states. Hence there is *always* a gap with the adjoining manifolds. This makes the extremal states generically robust for adiabatic passage.

The lower panel of Fig. 1 shows the NV spin coherence $\mathcal{L}(\tau) = \langle\hat{S}_x\rangle$ and nuclear bath polarization $\mathcal{P}(\tau) = \frac{1}{N_{\rm nuc}}\sum_n \frac{2}{\hbar}\langle\hat{I}_z^n\rangle$ as an adiabatic sweep over τ is carried out, using the common CPMG protocol.

The sweep inverts the entire nuclear bath: an initial down-polarized bath state $|X_\pm \downarrow^{(N_{\rm nuc})}\rangle$ follows the Floquet state trajectory to a fully up-polarized state $|X_\mp \uparrow^{(N_{\rm nuc})}\rangle$. Provided $t_{\rm tot} \lesssim T_2$, a coherent NV state evolves into another coherent NV state (from $|X_+\rangle$ to $|X_-\rangle$). This represents a type of gate, employing adiabatic passage, but on the underlying Floquet states.

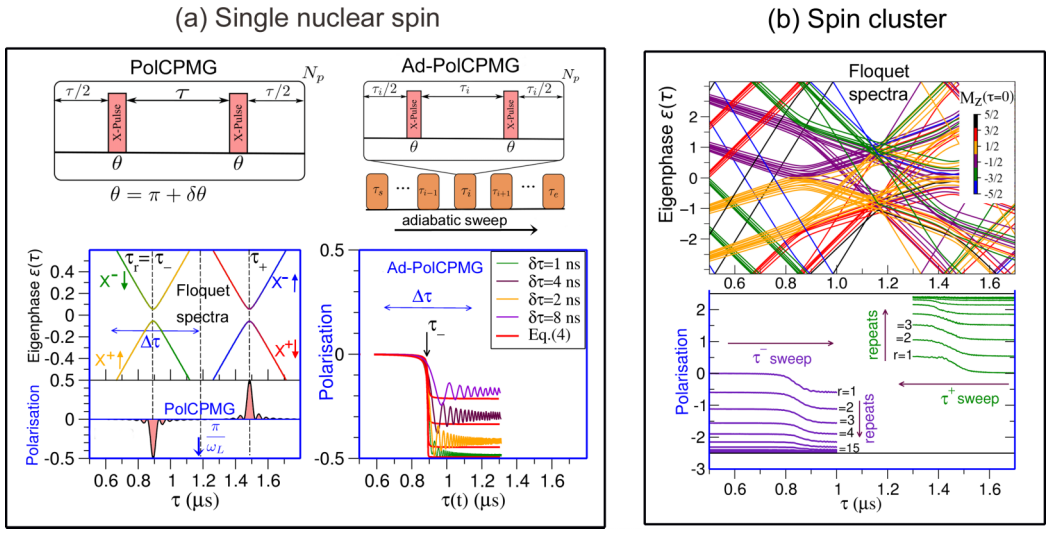

FIG. 2. Comparison of standard DD with ad-Pulse DD, exemplified by the PolCPMG polarization protocol, applied to an NV center electron coupled to one or more nuclear spins. In PolCPMG experiments [27], a slight under-/overrotation of the π pulses splits the normal CPMG resonance into two $\tau_r \equiv \tau^{\pm}$ resonances that are nuclear-state selective. The initial state is $|X^{\pm}\rangle\langle X^{\pm}|_{\rm NV} \otimes \rho_n$: The nuclei are initially in a mixed state and $|X^{\pm}\rangle \equiv \frac{1}{\sqrt{2}}[|0\rangle \pm |1\rangle]$. (a) Single spin case: DD resonances correspond to avoided crossings of the Floquet eigenphases (upper panel). For the standard case, N_p cycles of PolCPMG are applied at a single $\tau = \tau^-$ or τ^+; this polarizes the nuclei (lower panel). If a different τ is used, the NV is reinitialized. In contrast, for the corresponding ad-PolCPMG adiabatic protocol, one sweeps slowly over the range $\tau = \tau^{\pm} \pm \Delta\tau/2$ without reinitialization of the NV. As the step size, $\delta\tau$, is reduced, the sweep becomes adiabatic and full polarization is achieved: The behavior is well described by Eq. (4), based on Landau-Zener theory (red curves). (b) Multispin cluster: The Floquet level structure is illustrated for the case of $N_{\rm nuc} = 5$ nuclei. Although M_z is not a good quantum number during the ad-Pulse, for clarity, states are colored according to the asymptotic M_z at $\tau = 0$. Polarization can be achieved even by subadiabatic sweeps $\Gamma_0 < 1$ [see Eq. (4)], provided they are combined with repetitions where the NV state is reinitialized. For each repetition ($r = 1, 2...N_r = 15$ here), the polarization of the bath increases monotonically from zero initially. Full polarization is achieved for τ^- (lower panel), but for τ^+ the sweep saturates, possibly because the end points are not asymptotic. $N_s = 500$ and $\delta\tau = 1$ ns. Similar results are obtained for any subset of the $N_{\rm nuc} = 7$ spin cluster investigated here (further comparisons and coupling strengths are given in Table I in the Appendix).

IV. LANDAU-ZENER MODEL FOR AD-PULSE

We can apply LZ theory to analyze the adiabatic sweep, but need to adapt it to the Floquet eigenstate spectra. The sweep ranges from initial $\tau = \tau_{\rm ini}$ to a final $\tau_{\rm fin}$ and $\tau(t)$ must vary—in real time t—sufficiently slowly for adiabatic passage along $\mathcal{E}_l(\tau)$.

The range $\tau_{\rm ini} : \tau_{\rm fin}$ contains the anticrossing region near $\tau \simeq \tau_r$, but $\tau_{\rm ini}$, $\tau_{\rm fin}$ must both lie *outside* the anticrossing region. For a single nuclear spin, for any value of $\tau \in [\tau_{\rm ini} : \tau_{\rm fin}]$, we find the probability of losses from the eigenstate trajectory are given by $e^{-\Gamma_{LZ}(\tau(t))}$, where

$$\Gamma_{\rm LZ}(\tau(t)) = \frac{2A_x^2\tau_r^2 T_r}{\beta^2\delta\tau} F(\tau_{\rm ini}, \tau) \equiv \Gamma_0 F(\tau_{\rm ini}, \tau), \text{ where}$$
$$F(\tau_{\rm ini}, \tau) = \frac{1}{\pi}[\arctan(\Phi_\tau) - \arctan(\Phi_{\tau_{\rm ini}})] \quad (4)$$

and Γ_0 is the well-known LZ exponent (see Appendix for further details). $T_r = 4\tau_r$ for PulsePol, $T_r = 2\tau_r$ for CPMG or PolCPMG. $\Phi_\tau = \frac{4\pi(\tau-\tau_r)}{\tau}\sqrt{T_r/\delta\tau}$. As $\tau \to \tau_{\rm fin}$, then $F(\tau_{\rm ini}, \tau) \to 1$ and $\Gamma_{\rm LZ}(\tau(t)) \to \Gamma_0$. We can readily relate Eq. (4) to a corresponding nuclear polarization:

$$P_{\rm pol}(t) \simeq \pm(1 - e^{-\Gamma_{\rm LZ}(t)})/2, \quad (5)$$

here obtained as a closed-form expression in terms of the couplings A_z, A_x, sweep parameters and applied magnetic field, that are shown to be in good agreement with exact quantum numerics [see next section and Fig. 2(a)].

For adiabaticity (no losses), $\Gamma_0 \gg 1$; this requirement constrains $t_{\rm tot}$. However, the sweep range $\Delta\tau = \tau_{\rm fin} - \tau_{\rm ini}$ required is another important consideration; i.e., although $\Gamma_0 \propto A_x^2$, since $\Delta\tau \sim A_x$, we find the total time required increases linearly $t_{\rm tot} \propto A_x^{-1}$ (see Appendix for derivation). For optimized ad-Pulse, from Eq. (2), we can take $\tau_1 \equiv \tau_{\rm ini}$ and $\tau_{\rm fin} \equiv \tau_{N_s}$.

For adiabaticity, we also require a sufficiently small step-size $\delta\tau$. For $\Gamma_0 > 1$ (see Appendix), we require

$$\delta\tau \lesssim \frac{2A_x^2\tau_r^2 T_r}{\beta^2}. \quad (6)$$

β is a protocol dependent parameter. $\beta = (\pi + \delta\theta)$ for ad-PolCPMG/CPMG while $\beta = 6\pi/(2+\sqrt{2})$ for ad-PulsePol. A smaller step size may be achieved increasing N_p since effective step size $\delta\tau \to \delta\tau/N_p$ includes number of cycles. For ad-Pulse, in general $N_p = 1$, where N_p denotes the number of protocol cycles applied with the *same* τ, whereas the $k = 1, 2, ...N_s$ steps of the sweep all have a different τ. However, the sweep may be made slower or more adiabatic by increasing N_p.

V. AD-PULSE: NUCLEAR POLARIZATION

We now consider another application of ad-Pulse. In Fig. 1, it was assumed that the nuclei start from a pure, polarized

initial state. Generally, the nuclear bath is in a mixture; initializing the NV spin can be achieved optically and is comparatively straightforward. In Fig. 2, we show how ad-Pulse adiabatic sweeps with PolCPMG or PulsePol may also be used to prepare a pure initial nuclear state from a mixture. We show results for ad-PolCPMG, but ad-PulsePol yields similar behaviours.

Figure 2(a) (left panels) shows the Floquet spectrum for PolCPMG for a single spin with $\delta\theta = 0.25\pi$. The degeneracy of the level anticrossings in CPMG is lifted into two distinct crossings at $\tau^{\pm}$, and hence there are two coherence dips in the NV's trace. Applying PolCPMG at τ_- (τ_+) will target the $|\uparrow\rangle$ ($|\downarrow\rangle$) nuclear state and evolve it into the $|\downarrow\rangle$ ($|\uparrow\rangle$) state, polarizing the spin.

Figure 2(a) (right panels) shows the application of ad-PolCPMG to initialize a single spin and shows the polarization is well-described by Eq. (4): Full polarization is achieved when the sweep is adiabatic. In fact, if we allow repeated sweeps and/or reinitialization of the NV electron spin, we find the spin bath polarization is robust to a degree of nonadiabaticity. Furthermore, detailed comparisons with both ad-PulsePol and ad-PolCPMG are presented in the Appendix and show excellent agreement for all parameters.

Figure 2(b) examines the case of multiple nuclear spins. The right panel shows the multispin Floquet spectra. The levels group into manifolds of different M_z (for the five-spin case, $M_z = -5/2, -3/2 \ldots + 5/2$, and there are six manifolds). Hyperfine coupling only allows couplings (or avoided crossings) between neighboring M_z and $M_z \pm 1$ manifolds.

For the multispin ad-PolCPMG and the $\tau = \tau^-$ resonance, we find that about $N_r = 10-15$ repetitions is sufficient to fully polarize (>99.5%), whereas standard PolCPMG requires 100's of repeated sequences and NV reinitialization. For τ^+, a limit corresponding to about 95% polarization is reached, possibly because the initial and end states do not correspond to the asymptotic $|X^{\pm}\rangle|M_z\rangle$ basis. A sweep from $\tau = 0$ avoids these issues. Numerical tests were performed for clusters with $N_{\rm nuc} \leqslant 7$ and reasonable coupling strength $A_x \gtrsim$ 10 kHz, and showed broadly similar behavior. It is possible to investigate larger clusters, but the system dimensionality and computational cost increases rapidly with $N_{\rm nuc}$.

VI. AD-PULSE: QUANTUM GATES

We investigate ad-PulsePol for quantum state storage. The Floquet spectrum corresponding to the cluster of three nuclei C1-C3 is shown in Fig. 3, either as independent spins (top panel) or for the three-spin cluster (lower panel) for $B_0 = 0.0403$ T. For ad-PulsePol, plotting the eigenphases $\mathcal{E}_l \in [-\pi/2 : \pi/2]$ is most insightful, as it shows that the important crossings come in pairs. They are labeled for spin C2 (blue) for the third harmonic ($j = 3$ for τ_r) corresponding to $\hat{H}_{\rm PP} = gI^+S^-$. They show that an initial state $|1\downarrow\rangle \leftrightarrow |0\uparrow\rangle$, while $|1\uparrow\rangle \rightarrow |1\uparrow\rangle$ and $|0\downarrow\rangle \rightarrow |0\downarrow\rangle$.

We can show that an adiabatic sweep passing through such a pair of crossings would map an arbitrary initial NV state onto the nuclear spin state:

$$\begin{aligned}[a|0\rangle + b|1\rangle]_{\rm NV} \otimes |\downarrow\rangle_{\rm nuc} &\rightarrow |0\rangle_{\rm NV} \otimes [a|\downarrow\rangle + b|\uparrow\rangle]_{\rm nuc},\\ [a|0\rangle + b|1\rangle]_{\rm NV} \otimes |\uparrow\rangle_{\rm nuc} &\rightarrow |0\rangle_{\rm NV} \otimes [a|\downarrow\rangle + b|\uparrow\rangle]_{\rm nuc},\end{aligned} \tag{7}$$

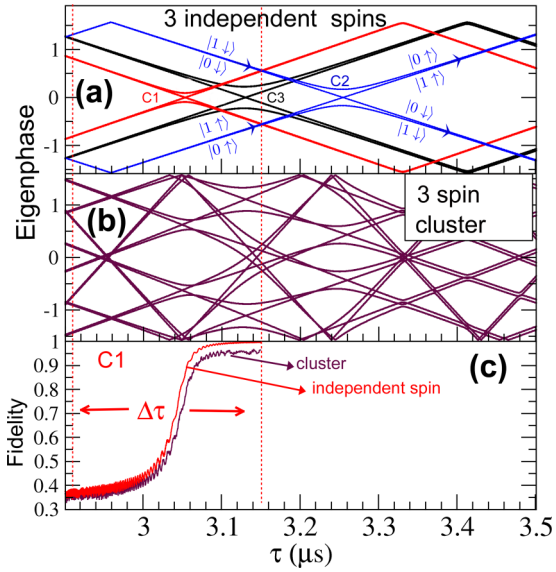

FIG. 3. Illustration of state storage and readout using the ad-PulsePol protocol. (a) The top panel shows the Floquet spectra for the three independent spins C1–C3. For this protocol, it is insightful to show eigenphases $\mathcal{E}_l \in [-\pi/2 : \pi/2]$ as the spectra show three pairs of crossings: Each of these corresponds to a true crossing superposed on an avoided crossing. (b) Spectra for the full three-nuclear spin dynamics. Each pair of crossings in (a) is now associated with a family of four anticrossings. A single ad-sweep over one of the crossings (we investigate the $\tau = 0.7 - 1.0$ μs range), transfers an arbitrary NV state $|\psi\rangle_{\rm NV} \otimes |\downarrow / \uparrow\rangle$ to a pure nuclear state, $|0/1\rangle_{\rm NV} \otimes |\psi\rangle_n$, within Larmor phases. (c) Shows the fidelity for transferring the NV state to nuclear spin C1 ($A_x = 26.6 \times 2\pi$ kHz) for the case where C1 is isolated (red line) and embedded in a three-spin cluster (maroon line).

noting that for the second line, the adiabatic sweep leaves the NV in the $|1\rangle$ state, so optical reinitialization to $|0\rangle$ is assumed. As usual for state storage in nuclear registers, since the relative nuclear phases rotate continuously as $e^{\pm i\omega_L t}$, required values are selected by timing the Larmor precession.

We test this for an adiabatic sweep over $\Delta\tau$ centered on τ_r for spin C1 ($A_x/(2\pi) \simeq 20$ kHz), starting with the test state $|\Psi_0\rangle = [\frac{1}{\sqrt{3}}|0\rangle + \frac{2}{\sqrt{3}}|1\rangle]_{\rm NV} \otimes |\downarrow\rangle_{\rm nuc}$ and testing the fidelity of the overlap $\mathcal{F}(\tau) = |\langle\Psi_0|\Psi_T\rangle|$ where $|\Psi_T\rangle = |0\rangle_{\rm NV} \otimes [\frac{1}{\sqrt{3}}|\downarrow\rangle + \frac{2}{\sqrt{3}}|\uparrow\rangle]_{\rm nuc}$, but disregarding phases between the nuclear states for convenience (by taking modulus of the coefficients of Ψ_T). Figure 3 (lower panel) shows that the partial overlap between avoided crossings reduces the fidelity appreciably, indicating that although this technique may be used, it is restricted to very well isolated (well-resolved in τ_r) nuclear spins. ad-PolCPMG can equally achieve an equivalent state storage gate.

VII. DISCUSSION AND CONCLUSIONS

In this paper, we introduced the technique of adiabatic pulse-based DD control (ad-Pulse). We show it has a broad range of potential applications that opens several avenues for experimental studies, ranging from polarization and initialization of nuclear mixtures to control of single multispin pure states for state storage and preparation.

To motivate ad-Pulse, it is legitimate to ask what advantages it might add to the family of standard DD control protocols already available? We investigated two scenarios:

First, as Fig. 1 illustrates, ad-Pulse opens the possibility of control of pure states via adiabatic passage, showing the effects are readily visualized as a trajectory in the eigenphase spectra. While two specific illustrations are presented here (Figs. 1 and 3), the possibilities are far from exhausted as protocols other than CPMG may have gapped states that are robust to adiabatic passage or isolated spins (for state storage illustrated in Fig. 3). For an adiabatic gate, both the NV and nuclei have been prepared in an initial pure state, that ad-Pulse evolves and/or steers by adiabatic passage to another pure state of interest. This will introduce an additional challenge. As the adiabatic passage would not use repetitions, for good fidelities, it must be concluded within the coherence time $T_2 \sim$ ms.

Second, there are applications such as polarization of nuclear mixtures. Here, the ability to use repetitions, where one reinitializes the NV in a coherent state, while the long-lived nuclear bath starts in an already partially polarized state in subsequent sweeps, renders the requirement to complete the sweep within the T_2 time less onerous.

One motivator for new techniques is that recent studies on nuclear registers involve clusters of multiple nuclei where, even in the absence of significant many-body nuclear-nuclear coupling, there is the challenge of dealing with a scenario of multiple overlapping resonances (even more so in the protocols that split the resonances for nuclear state selectivity). Polarization protocols using single $\tau \simeq \pi/\omega_L$ will necessarily drive some of the spins off-resonance, and previous studies have identified the formation of dark states that can cause hyperpolarization to saturate well below the maximum. As a result, imperfect polarization results. While of less significance where NMR signal enhancement is the goal, imperfect polarization 90−99% may be inadequate for state storage and quantum information.

ad-Pulse sweeps gradually over the entire resonance region containing multiple resonant spacings $\tau_1, \tau_2 ... \tau_{N_{\rm nuc}}$. Numerical simulations indicate that it can yield better polarization saturations. However, there are constraints: ad-Pulse works less well for weaker coupled nuclei $A_x \ll 10$ kHz as the adiabatic sweep time becomes slow compared with T_2. Another constraint is that the adiabatic sweep must begin at initial and final τ far from any avoided crossing: In Fig. 2(b), this effect is already apparent in the τ_+ sweep as that yields lower saturation polarizations. In terms of a comparison for the time taken, PolCPMG or PulsePol will use $N_p \sim 10-100$, while $N_r \sim 100-1000$. In contrast, ad-CPMG (in Fig. 2) employed $N_s \sim 1000$, while $N_r \sim 10$. Thus the total time to achieve polarization saturation is comparable. Future experimental studies will be required to undertake more definitive comparisons, including the decohering effect of the distant bath of weakly coupled nuclei.

ACKNOWLEDGMENTS

The authors thank Conor Bradley and Asier Galicia for useful discussions. O.W. acknowledges support from DTP studentship grant EP/R513143/1 of the Engineering and Physical Sciences Research Council (EPSRC). This work was supported by the Netherlands Organisation for Scientific Research (NWO/OCW) through a Vidi grant and as part of the Frontiers of Nanoscience (NanoFront) program and the Quantum Software Consortium program (Project No. 024.003.037/3368). This project has received funding from the European Research Council (ERC) under the European Union's Horizon 2020 research and innovation program (Grant Agreement No. 852410).

APPENDIX

1. Adiabatic DD dynamics: single spin analysis

Under common DD control sequences, the joint NV electronic-nuclear spin system is associated with resonant frequencies, $\omega_r = \pi/\tau_r$, where τ_r are resonant pulse spacings at which the electron-nuclear spins entangle. The ω_r are characteristic to each nucleus: For example, CPMG has resonances at $\tau_r = \pi/\omega_I$, where $\omega_I = \omega_L + A_z/2$ and A_z is the parallel hyperfine coupling strength for a particular nucleus while ω_L is the Larmor frequency. There is often a sharp dip in the measured coherence of the NV, at $\tau = \tau_r$, that forms the basis of DD-based nuclear sensing.

For the polarization protocols PolCPMG and PulsePol [25,27], there is instead a pair of resonant $\tau_r^{\pm}$ on either site of $\tau = \pi/\omega_I$ where the entanglement dynamics affects either the up or down nuclear states specifically. PolCPMG is a comparatively minor variation on the well-known CPMG protocol. CPMG is a two-π-pulse sequence, $[\frac{\tau}{2} - \pi_x - \tau - \pi_x - \frac{\tau}{2}]^{N_p}$, where N_p represents the number of times the cycle is applied. For PolCPMG, a small pulse over-/underrotation is introduced. Hence, instead of employing a $\theta = \pi$ pulse, one employs $\theta = \pi + \delta\theta$. This may be implemented experimentally by slightly lengthening/shortening the pulse duration T_p, yielding resonances at

$$\tau_r^{\pm} = \frac{\pi \pm \delta\theta}{\omega_I} \text{ and } \delta\theta = \pi \frac{T_p - T_\pi}{T_\pi}, \tag{A1}$$

as well as odd multiples of τ_r. Here T_π is the duration of a π pulse. The total protocol period is $T = 2\tau + 2T_p$. However, as the spin-selective dynamics depend only on $\delta\theta$, in our calculations, we assume very short pulses $T_p \to 0$ and thus $T = 2\tau$. Finite duration pulses are also of interest as these can give rise to new types of resonances at even-integer multiples of τ_r [30], but such effects are not considered here.

PulsePol involves a more complex sequence of pulses [25] of the form $[\frac{\pi_y}{2} - \tau - \pi_{-x} - \tau - \frac{\pi_y}{2}\frac{\pi_x}{2} - \tau - \pi_y - \tau - \frac{\pi_x}{2}]^{2N_p}$. The sequence was shown in Ref. [25] to yield effective flip-flop Hamiltonians $\hat{H}_{\rm PP} = gI^{\pm}S^{\mp}$ at $\tau_r^{\pm}$ respectively. Although resonances occur at all odd harmonics, the strongest is at pulse interval $\tau_r = \tau^+ = \frac{3\pi}{2\omega_I}$. The total period of the PulsePol protocol sequence is $T = 4\tau$.

The polarization time $t_{\rm pol}$, i.e., the time needed to rotate an up nuclear state into a down nuclear state, or vice versa, was obtained in previous studies [25,27],

$$t_{\rm pol} = \frac{\pi(\pi + \delta\theta)}{A_x \cos\delta\theta/2} \text{ (PolCPMG)},$$
$$t_{\rm pol} = \frac{2\pi}{A_x \alpha}, \quad \alpha = \frac{2(2+\sqrt{2})}{3\pi}; \quad \text{(PulsePol)}, \tag{A2}$$

where A_x is the perpendicular component of the hyperfine coupling. In Refs. [26,27], it was shown that on resonance, at pulse intervals $\tau = \tau_r^{\pm}$, there are avoided crossing in the underlying Floquet eigenspectra, involving two specific eigenstates. They are associated with Rabi oscillations of frequency Ω between the up/down nuclear spin states, where $\Omega = \pi/t_{\rm pol}$. Thus, applying DD at $\tau = \tau_r^{\pm}$ polarizes a nucleus initially in a spin mixture. For CPMG, $\tau_r^+ = \tau_r^-$, both crossings are degenerate so no polarization is obtained.

For their adiabatic-DD counterparts, knowledge of the Floquet eigenstates on either side of the crossings enables one to guide eigenstates adiabatically along the desired state trajectory. ad-PulsePol or ad-PolCPMG/CPMG were analyzed in detail in this paper, but other protocols can be treated similarly. For the adiabatic-pulse (ad-Pulse) sweeps, the sweep is over a τ region that *contains* the interaction region i.e., the avoided crossing region surrounding the τ_r of interest. The initial points $\tau_{\rm ini}$ and final point $\tau_{\rm fin}$, however, should lie outside, and on either side of, the interaction region: The width of the sweep $\Delta\tau = |\tau_{\rm fin} - \tau_{\rm ini}|$, should considerably exceed the width of the avoided crossing.

We define a detuning from resonance:

$$\Delta_D(\tau) = \omega_r - \omega(\tau) \equiv \frac{\pi}{\tau_r} - \frac{\pi}{\tau}, \tag{A3}$$

noting that $\Delta_D(\tau) \equiv \Delta_D(\tau(t))$ as τ is swept in time, we also define a rate of the sweep or level velocity:

$$\begin{aligned} \dot{\Delta}_D(\tau(t)) &= \frac{\pi}{\tau^2}\frac{d\tau}{dt}, \quad \text{hence} \\ \dot{\Delta}_D(\tau_r) &= \frac{\pi\delta\tau}{N_p\tau_r^2 T_r}, \end{aligned} \tag{A4}$$

since $\frac{d\tau}{dt}|_{\tau_r} \simeq \delta\tau/(N_p T_r)$ and the protocol period at resonance $T_r = 2\tau_r$ for ad-PolCPMG but $T_r = 4\tau_r$ for ad-PulsePol. N_p is the number of cycles of the protocol at each value of τ, while $\delta\tau$ is the step size in τ. The experimental sweep employs discrete time steps where $N_s = \Delta\tau/\delta\tau \gg 1$ as $\delta\tau$ is small. We note that if the chosen $\delta\tau$ becomes too small for experimental electronics, one can in general adopt an effective step size $\delta\tau \to \delta\tau/N_p$. Below we set $N_p = 1$ and assume that the number of cycles is incorporated in the step size $\delta\tau$.

The polarization process starts with a nucleus in a mixed state so $\langle\hat{I}_z\rangle = 0$. If we wish to polarize into, say, the down state, we sweep over the region near $\tau = \tau_r^-$, where initial states with $\langle\hat{I}_z\rangle = -1/2$ remain unperturbed, while those for which initially $\langle\hat{I}_z\rangle = +1/2$ are involved in the avoided crossing. One can apply LZ theory to analyze the dynamics and compare with full quantum numerics for the sweep over this avoided crossing.

In LZ theory [34], the probability P_0 of remaining in the initial state in a given infinitesimal time interval δt depends on the transition rate $\Gamma(t)$ out of that state, thus

$$P_0(t+\delta t) = (1-\Gamma(t))P_0(t) \simeq e^{-\Gamma(t)}P_0(t). \tag{A5}$$

The state dynamics is characterized by an equation that takes $P_0(t = t_{\rm ini}) = 1$ to $P_0(t) \gtrsim 0$ at some final time $t_{\rm fin}$ so the transition rates are integrated in time:

$$P_0(t) = e^{-\int_{t_{\rm ini}}^{t}\Gamma(t)dt} = e^{-\Gamma_{\rm LZ}(t)}. \tag{A6}$$

In Ref. [34], a simple model adopts the Lorentzian form for the transition rate $\Gamma(t) = \Omega^2\frac{\gamma}{\Delta_D^2+\gamma^2}$. The parameter γ was analyzed in Ref. [34]: $\gamma^{-1} \sim T_d$ represents the characteristic dephasing time T_d of the sweep, i.e., the time to accumulate a phase difference of 2π between neighboring segments (in τ). A heuristic analysis resulted in the form $\gamma \sim \sqrt{\dot{\Delta}_D/(4\pi)}$. We adopt this form and found it to be remarkably effective, hence we use

$$\gamma/2 = \sqrt{\frac{\dot{\Delta}_D(\tau_r)}{(4\pi)}} = \frac{1}{2}\sqrt{\frac{\delta\tau}{4T_r\tau_r^2}}. \tag{A7}$$

$\Gamma(t)$ may be analytically integrated up to some arbitrary final time t, so

$$\Gamma_{\rm LZ}(t) = \frac{2\Omega^2}{\dot{\Delta}_D(\tau_r)}\left[\arctan\frac{\Delta_D(\tau)}{\gamma/2} - \arctan\frac{\Delta_D(\tau_0)}{\gamma/2}\right]. \tag{A8}$$

The function $\Gamma_{\rm LZ}(t)$ may be written in the form

$$\begin{aligned} \Gamma_{\rm LZ}(t) &= \Gamma_0 F(t_{\rm ini}, t), \ \text{with} \\ \Gamma_0 &= \frac{2\pi\Omega^2}{\dot{\Delta}_D(\tau_r)} \end{aligned} \tag{A9}$$

and where

$$F(t_{\rm ini}, t) = \frac{1}{\pi}\left[\arctan\frac{\Delta_D(\tau(t))}{\gamma/2} - \arctan\frac{\Delta_D(\tau_0)}{\gamma/2}\right] \tag{A10}$$

interpolates from $F = 0$ at $t = t_{\rm ini}$ to $F = 1$ as $t \to \infty$.

We note that when $\Delta_D(\tau = \tau_{\rm fin}) \gg \gamma \gg \Delta_D(\tau_{\rm ini})$, the resonant region around τ_r is well contained within the range $\tau \in [\tau_{\rm ini} : \tau_{\rm fin}]$, then

$$\Gamma_{\rm LZ}(t) \to \Gamma_0, \tag{A11}$$

and thus the probability of remaining in the initial state is $P_0 = e^{-\Gamma_0}$, is independent of γ, and is given only by Γ_0, the LZ exponent. The probability of adiabatically following the trajectory is $1 - P_0$: conversely, P_0 denotes the probability of *losses* from the adiabatic trajectory. Γ_0 quantifies the degree of adiabaticity of a parameter sweep along an eigenstate trajectory.

For our present example of an initial spin in $m_I = +1/2$, if $\Gamma_0 \gg 1$, then $P_0 \simeq 0$ and no probability remains in the initial state; the spin has flipped to $m_I = -1/2$ and is fully polarized as the sweep is adiabatic. The calculated polarization is given by $P_{\rm pol}(t) = \pm(1 - e^{-\Gamma_{LZ}(t)})/2$ (depending on whether we are using τ_r^+ or τ_r^-). We use $\mathcal{P}$ to denote the polarization of the initial nuclear mixture, so in Fig. 4 we compare $P_0(t)$ calculated analytically (red lines) with full numerical calculations of $1 + 2\mathcal{P}$ for τ_r^- (PolCPMG) or $1 - 2\mathcal{P}$ for τ_r^+ (PulsePol) .

We can substitute Eqs. (A2) and (A4) into Eq. (A9) to obtain

$$\begin{aligned} P_0(t) &= e^{-\Gamma_{LZ}(\tau(t))}, \ \text{where} \\ \Gamma_{\rm LZ}(\tau(t)) &= \Gamma_0 F(t_0, t) = \frac{2A_x^2\tau_r^2 T_r}{\beta^2\delta\tau}F(t_0, t), \end{aligned} \tag{A12}$$

where $\beta = (\pi + \delta\theta)$ for PolCPMG while $\beta = 6\pi/(2+\sqrt{2})$ for PulsePol. The time dependence of the polarization, $F(t_0, t_f)$, is readily evaluated using Eqs. (A7) and Eq. (A4).

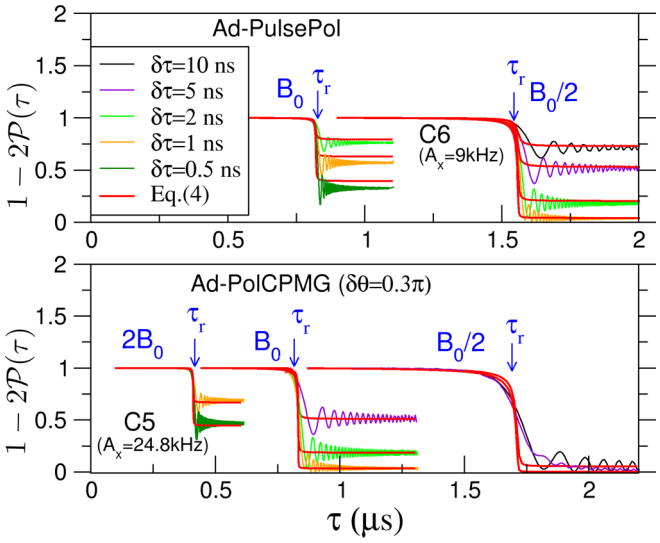

FIG. 4. Shows that the Landau-Zener theory Eq. (4) in the main text reproduces the spin-flip behavior of adiabatic sweeps for different spin coupling, magnetic field strengths, and different protocols. $B_0 = 0.0403$ T. The colored lines represent quantum calculations for different step sizes $\delta\tau$: As the Landau-Zener exponent Γ_0 increases, the fidelity of the adiabatic trajectory increases. The red lines overlaid correspond to $P_0 = \exp[-\Gamma_{\rm LZ}(\tau)]$ given by Eq. (4) in the main text or Eq. ((A13)) here. Agreement for ad-PolCPMG is excellent; for the ad-PulsePol protocol, as the magnetic field increases, the Landau-Zener theory acquires an asymptotic offset from the quantum results of 10–20%, but still predicts quite reliably which step sizes will yield an adiabatic, high fidelity sweep (thus $P_0 \to 0$ at the end of the sweep).

Finally, we substitute Eqs. (A7) and (A3) into the form of $F(t_0, t_f)$ to obtain

$$\Gamma_{\rm LZ}(\tau) = \frac{2A_x^2\tau_r^2 T_r}{\beta^2\delta\tau}\frac{1}{\pi}[\arctan\Phi_\tau - \arctan\Phi_{\tau_{\rm ini}}], \quad \text{(A13)}$$

with $\Phi_\tau = \frac{4\pi(\tau-\tau_r)}{\tau}\sqrt{T_r/\delta\tau}$ which corresponds to the form of $\Gamma_{\rm LZ}(\tau(t))$ Eq. (4) in the main text.

In Fig. 4, we test the LZ theory for different magnetic fields, coupling strengths, and protocols, and show it reliably quantifies adiabaticity for a wide range of parameters.

2. Adiabatic gate time $t_{\rm tot}$

From the above, we see that an adiabatic sweep that will transfer an initial state to the final state along an eigenstate requires that

$$\Gamma_0 = \frac{2A_x^2\tau_r^2 T_r}{\beta^2\delta\tau} \gtrsim 1; \quad \text{(A14)}$$

hence for a given magnetic field strength and hyperfine coupling, we require that the step size be smaller than

$$\delta\tau_{\rm max} = \frac{2A_x^2\tau_r^2 T_r}{\beta^2}. \quad \text{(A15)}$$

The total number of steps needed is thus $N_{\rm steps} = (\tau_{\rm fin} - \tau_{\rm ini})/\delta\tau = \Delta\tau/\delta\tau_{\rm max}$ and the total gate time needed is

$$t_{\rm tot} = \frac{\Delta\tau}{\delta\tau_{\rm max}}T_r \quad \text{(A16)}$$

TABLE I. Nuclear spins: Hyperfine coupling strengths.

Spin	$A_z/(2\pi)$ (kHz)	$A_x/(2\pi)$ (kHz)
C1	−36.308	26.62
C2	20.569	41.51
C3	−11.346	59.21
C4	8.029	21.0
C5	24.399	24.81
C6	−48.58	9.0
C7	−20.72	12.0

(we recall the effective step $\delta\tau \to \delta\tau/N_p$ includes number of cycles).

3. Estimate range of the adiabatic sweep: $\Delta\tau$

To obtain an estimate of $\Delta\tau$, we employ a sweep that contains the resonance thus ranges from an initial $\tau_{\rm ini} \approx \tau_r - \Delta\tau/2$ to a final $\tau_{\rm fin} \approx \tau_r + \Delta\tau/2$.

The parameter γ may be used to estimate the width of the interaction region. The time-dependence envelope ranges from a value $F(t_0, t) = 0$ at $\tau = \tau_{\rm ini}$ to $F(t_0, t) = 1$ at $\tau = \tau_{\rm fin}$. We can define a representative middle region bounded by

$$\arctan(\Delta_D(\tau)/(\gamma/2)) \sim \pm\pi/4. \quad \text{(A17)}$$

Hence

$$\Delta_D(\tau) = \pi\frac{\tau-\tau_r}{\tau\tau_r} \simeq \gamma = \sqrt{\frac{\delta\tau}{4T_r\tau_r^2}} \quad \text{(A18)}$$

or

$$\Delta_D(\tau) = \pi\frac{\tau-\tau_r}{\tau\tau_r} \simeq \pi\Delta\tau_m/\tau_r^2, \quad \text{(A19)}$$

using $\delta\tau \equiv \delta\tau_{\rm max}$, we obtain

$$\Delta\tau_m \simeq \tau_r^2 A_x\frac{\sqrt{2}}{\beta\pi}. \quad \text{(A20)}$$

However, the width of the adiabatic sweep has to considerably exceed the inner width of the resonance to ensure that the states start and end at their asymptotic values, hence $\Delta\tau \gg \Delta\tau_m$.

We find that a good value is to take

$$\Delta\tau/2 = C_\Delta\frac{\tau_r^2 A_x}{\beta}, \quad \text{(A21)}$$

with $C_\Delta \sim 6$. The τ sweep should be as wide as possible; however, if it is too wide, the $\tau \in [\tau_{\rm ini} : \tau_{\rm fin}]$ region may begin to overlap with neighboring crossings, even for a well-isolated spin. In addition, since the gate time $t_{\rm tot}$ scales as $\Delta\tau$, if possible, the lowest value required to ensure the required fidelity should be chosen.

Combining Eq. (A16) with Eqs. (A21) and (A15), we obtain

$$t_{\rm tot} \simeq \beta/A_x. \quad \text{(A22)}$$

In other words, if the sweep range can be optimized and scaled appropriately for different magnetic fields, the gate time varies as A_x^{-1}. However, for a spin cluster covering a

range of A_x this may not be possible to a full extent. Nevertheless, interestingly, one may adjust the sweep range to make the gate time independent of the magnetic field strength as there is no dependence on τ_r.

The total time taken for the gate is found by taking the summation over all time steps to obtain

$$t_{\rm tot} = T_r\left(\frac{\Delta\tau}{\delta\tau}+1\right) \simeq T_r\frac{\Delta\tau}{\delta\tau}. \tag{A23}$$

Assuming that for a highly adiabatic sweep $\Gamma_0 \sim 5-7 \equiv C_\delta^{-1}$, then

$$\delta\tau = C_\delta\frac{2A_x^2\tau_r^2T_r}{\beta^2}. \tag{A24}$$

For this case, then the total gate time is

$$t_{\rm tot} = \frac{C_\Delta}{C_\delta}\frac{\beta}{A_x}. \tag{A25}$$

In Fig. 5, for a highly adiabatic sweep (small C_δ), we compare the effect of varying the sweep range $\Delta\tau$, showing that $C_\Delta \sim 4-6$ yields converged results.

Although the LZ approach is remarkably reliable in describing the transition to adiabaticity $0 \lesssim \Gamma_0 \lesssim 10$, once the sweep is at the adiabatic limit, the full quantum dynamics saturates: There is a perfect evolution from the initial to the final quantum state. The LZ exponentiation $e^{-\Gamma_0}$, however, behaves unphysically for large Γ_0. Adiabatic methods may also be investigated in combination with pulse-based Hamiltonians designed for many-body spin systems [35].

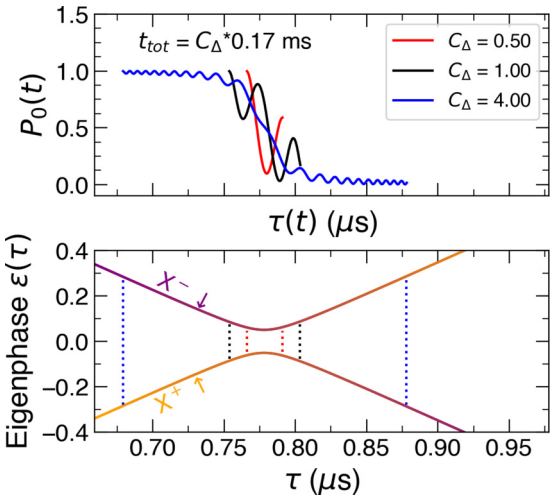

FIG. 5. Upper panel: An adiabatic sweep of the single spin, C1, under a static magnetic field of $B_0 = 0.0403$ T for different values of C_Δ and hence a range of $\Delta\tau$'s. To indicate where the sweep starts in relation to the Floquet spectrum, the lower panel displays the single-spin Floquet phases for C1 with the range of $\Delta\tau$'s highlighted as colored dotted lines. A larger C_Δ leads to a smoother adiabatic sweep, but this linearly increases the total sweep time, $t_{\rm tot}$. We take $C_\delta = 1/7$ and very good results are obtained already for $C_\Delta = 4$ with reasonable results achieved for $C_\Delta \gtrsim 2$.

[1] R. Schirhagl, K. Chang, M. Loretz, and C. L. Degen, Nitrogen-vacancy centers in diamond: Nanoscale sensors for physics and biology, Annu. Rev. Phys. Chem. **65**, 83 (2014).

[2] F. Jelezko, T. Gaebel, I. Popa, M. Domhan, A. Gruber and J. Wrachtrup, Observation of Coherent Oscillation of a Single Nuclear Spin and Realization of a Two-Qubit Conditional Quantum Gate, Phys. Rev. Lett. **93**, 130501 (2004).

[3] L. Childress, M. V. Gurudev Dutt, J. M. Taylor, A. S. Zibrov, F. Jelezko, J. Wrachtrup, P. R. Hemmer, and M. D. Lukin, Coherent dynamics of coupled electron and nuclear spin qubits in diamond, Science **314**, 281 (2006).

[4] J. R. Maze, P. L. Stanwix, J. S. Hodges, S. Hong, J. M. Taylor, P. Cappellaro, L. Jiang, M. V. Gurudev Dutt, E. Togan, A. S. Zibrov, A. Yacoby, R. L. Walsworth, and M. D. Lukin, Nanoscale magnetic sensing with an individual electronic spin in diamond, Nature **455**, 644 (2008).

[5] G. Balasubramanian, I. Y. Chan, R. Kolesov, M. Al-Hmoud, J. Tisler, C. Shin, C. Kim, A. Wojcik, P. R. Hemmer, A. Krueger, T. Hanke, A. Leitenstorfer, R. Bratschitsch, F. Jelezko, and J. Wrachtrup, Nanoscale imaging magnetometry with diamond spins under ambient conditions, Nature **455**, 648 (2008).

[6] T. Muller, C. Hepp, B. Pingault, E. Neu, S. Gsell, M. Schreck, H. Sternschulte, D. Steinmuller-Nethl, C. Becher and M. Atature, Optical signatures of silicon-vacancy spins in diamond, Nat. Commun. **5**, 3328 (2014).

[7] J. Hansom, C. H. H. Schulte, C. Le Gall, C. Matthiesen, E. Clarke, M. Hugues, J. M. Taylor and M. Atature, Environment-assisted quantum control of a solid-state spin via coherent dark states, Nat. Phys. **10**, 725 (2014).

[8] J. Cai, F. Jelezko, M. B. Plenio, and A. Retzker, Diamond-based single-molecule magnetic resonance spectroscopy, New J. Phys. **15**, 013020 (2013).

[9] C. Muller, X. Kong, J.-M. Cai, K. Melentijevic, A. Stacey, M. Markham, D. Twitchen, J. Isoya, S. Pezzagna, J. Meijer, J. F. Du, M. B. Plenio, B. Naydenov, L. P. McGuinness, and F. Jelezko, Nuclear magnetic resonance spectroscopy with single spin sensitivity, Nat. Commun. **5**, 4703 (2014).

[10] N. Zhao, J. L. Hu, S. W. Ho, J. T. K. Wan, and R. B. Liu, Atomic-scale magnetometry of distant nuclear spin clusters via nitrogen-vacancy spin in diamond, Nat. Nanotechnol. **6**, 242 (2011).

[11] N. Zhao, J. Honert, B. Schmid, M. Klas, J. Isoya, M. Markham, D. Twitchen, F. Jelezko, R.-B. Liu, H. Fedder and J. Wrachtrup, Sensing single remote nuclear spins, Nat. Nanotechnol. **7**, 657 (2012).

[12] F. Shi, X. Kong, P. Wang, F. Kong, N. Zhao, R.-B. Liu, and J. Du, Sensing and atomic-scale structure analysis of single nuclear-spin clusters in diamond, Nat. Phys. **10**, 21 (2014).

[13] P. Cappellaro, L. Jiang, J. S. Hodges and M. D. Lukin, Coherence and Control of Quantum Registers Based on Electronic Spin in a Nuclear Spin Bath, Phys. Rev. Lett. **102**, 210502 (2009).

[14] P. Neumann, R. Kolesov, B. Naydenov, J. Beck, F. Rempp, M. Steiner, V. Jacques, G. Balasubramanian, M. L. Markham, D. J. Twitchen, S. Pezzagna, J. Meijer, J. Twamley, F. Jelezko, and

J. Wrachtrup, Quantum register based on coupled electron spins in a room-temperature solid, Nat. Phys. **6**, 249 (2010).

[15] H. Bernien, B. Hensen, W. Pfaff, G. Koolstra, M. S. Blok, L. Robledo, T. H. Taminiau, M. Markham, D. J. Twitchen, L. Childress, and R. Hanson, Heralded entanglement between solid-state qubits separated by three metres, Nature (London) **497**, 86 (2013).

[16] N. Bar-Gill, L. M. Pham, A. Jarmola, D. Budker and R. L. Walsworth, Solid-state electronic spin coherence time approaching one second, Nat. Commun. **4**, 1743 (2013).

[17] S. Kolkowitz, Q. P. Unterreithmeier, S. D. Bennett and M. D. Lukin, Sensing Distant Nuclear Spins with a Single Electron Spin, Phys. Rev. Lett. **109**, 137601 (2012).

[18] T. H. Taminiau, J. J. T. Wagenaar, T. van der Sar, F. Jelezko, V. V. Dobrovitski, and R. Hanson, Detection and Control of Individual Nuclear Spins Using a Weakly Coupled Electron Spin, Phys. Rev. Lett. **109**, 137602 (2012).

[19] T. H. Taminiau, J. Cramer, T. van der Sar, V. V. Dobrovitski, and R. Hanson, Universal control and error correction in multi-qubit spin registers in diamond, Nat. Nanotechnol. **9**, 171 (2014).

[20] C. E. Bradley, J. Randall, M. H. Abobeih, R. C. Berrevoets, M. J. Degen, M. A. Bakker, M. Markham, D. J. Twitchen, and T. H. Taminiau, A Ten-Qubit Solid-State Spin Register with Quantum Memory up to One Minute, Phys. Rev. X **9**, 031045 (2019).

[21] N. Aslam, M. Pfender, P. Neumann, R. Reuter, A. Zappe, F. F. de Oliveira, A. Denisenko, H. Sumiya, S. Onoda, J. Isoya, and J. Wrachtrup, Nanoscale nuclear magnetic resonance with chemical resolution, Science **357**, 67 (2017).

[22] B. B. Zhou, A. Baksic, H. Ribeiro, C. G. Yale, F. Joseph Heremans, P. C. Jerger, A. Auer, G. Burkard, A. A. Clerk, and D. D. Awschalom, Accelerated quantum control using superadiabatic dynamics in a solid-state lambda system, Nat. Phys. **13**, 330 (2017).

[23] G. Quiroz and D. A. Lidar, High-fidelity adiabatic quantum computation via dynamical decoupling Phys. Rev. A **86**, 042333 (2012).

[24] W. M. Witzel, I. Montano, R. P. Muller, and M. S. Carroll, Multiqubit gates protected by adiabaticity and dynamical decoupling applicable to donor qubits in silicon, Phys. Rev. B **92**, 081407(R) (2015).

[25] I. Schwartz, J. Scheuer, B. Tratzmiller, S. Muller, Q. Chen, I. Dhand, Z.-Y. Wang, C. Muller, B. Naydenov, F. Jelezko, and M. B. Plenio, Robust optical polarization of nuclear spin baths using Hamiltonian engineering of nitrogen-vacancy center quantum dynamics, Sci. Adv. **4**, eaat8978 (2018).

[26] J. E. Lang, J.-P. Tetienne, and T. S. Monteiro, Dynamical decoupling protocols with nuclear spin state selectivity, arXiv:1810.00174.

[27] J. E. Lang, D. A. Broadway, G. A. L. White, L. T. Hall, A. Stacey, L. C. L. Hollenberg, T. S. Monteiro, and J.-P. Tetienne, Quantum Bath Control with Nuclear Spin State Selectivity via Pulse-Adjusted Dynamical Decoupling, Phys. Rev. Lett. **123**, 210401 (2019).

[28] K. O. Tan, C. Yang, R. T. Weber, G. Mathies, and R. G. Griffin, Time-optimized pulsed dynamic nuclear polarization, Sci. Adv. **5**, eaav6909 (2019).

[29] J. E. Lang, R. B. Liu, and T. S. Monteiro, Dynamical-Decoupling-Based Quantum Sensing: Floquet Spectroscopy, Phys. Rev. X **5**, 041016 (2015).

[30] J. E. Lang, J. Casanova, Z-Y. Wang, M. B. Plenio, and T. S. Monteiro, Enhanced Resolution in Nanoscale NMR via Quantum Sensing with Pulses of Finite Duration, Phys. Rev. Appl. **7**, 054009 (2017).

[31] A. Schmidt and S. Vega, The Floquet theory of nuclear magnetic resonance spectroscopy of single spins and dipolar coupled spin pairs in rotating solids, J. Chem. Phys. **96**, 2655 (1992); T. O. Levante, M. Baldus, B. H. Meier, and R. R. Ernst, Formalized quantum mechanical Floquet theory and its application to sample spinning in nuclear magnetic resonance, Mol. Phys. **86**, 1195 (1995); A. Schweiger and G. Jeschke, *Principles of Pulse Electron Paramagnetic Resonance* (Oxford University Press, Oxford, 2001).

[32] J. H. Shirley, Solution of the Schrödinger equation with a Hamiltonian periodic in time, Phys. Rev. **138**, B979 (1965).

[33] T. Villazon, P. W. Claeys, Anatoli Polkovnikov, and Anushya Chandran, Shortcuts to dynamic polarization, Phys. Rev. B **103**, 075118 (2021).

[34] A. C. Vutha, A simple approach to the Landau-Zener formula, Eur. J. Phys. **31**, 389 (2010).

[35] J. Choi, H. Zhou, H. S. Knowles, R. Landig, S. Choi, and M. D. Lukin, Robust Dynamic Hamiltonian Engineering of Many-Body Spin Systems, Phys. Rev. X **10**, 031002 (2020).